

REPORT

## PP2A regulates kinetochore-microtubule attachment during meiosis I in oocyte

An Tang<sup>a,#</sup>, Peiliang Shi<sup>a,#</sup>, Anying Song<sup>a,#</sup>, Dayuan Zou<sup>a,#</sup>, Yue Zhou<sup>b</sup>, Pengyu Gu<sup>c</sup>, Zan Huang<sup>d</sup>, Qinghua Wang<sup>a</sup>, Zhaoyu Lin<sup>a</sup>, and Xiang Gao<sup>a</sup>

<sup>a</sup>State Key Laboratory of Pharmaceutical Biotechnology and MOE Key Laboratory of Model Animal for Disease Study, Model Animal Research Center, Nanjing Biomedical Research Institute, Collaborative Innovation Center of Genetics and Development, Nanjing University, Nanjing, China; <sup>b</sup>State Key Laboratory of Food Science and Technology, Jiangnan University, Wuxi, China; <sup>c</sup>Neurobiology Department, University of Massachusetts Medical School, Worcester, MA, USA; <sup>d</sup>College of Animal Science & Technology, Nanjing Agricultural University, Nanjing, China

### ABSTRACT

Studies using *in vitro* cultured oocytes have indicated that the protein phosphatase 2A (PP2A), a major serine/threonine protein phosphatase, participates in multiple steps of meiosis. Details of oocyte maturation regulation by PP2A remain unclear and an *in vivo* model can provide more convincing information. Here, we inactivated PP2A by mutating genes encoding for its catalytic subunits (PP2Ac) in mouse oocytes. We found that eliminating both PP2Ac caused female infertility. Oocytes lacking PP2Ac failed to complete 1<sup>st</sup> meiotic division due to chromosome misalignment and abnormal spindle assembly. In mitosis, PP2A counteracts Aurora kinase B/C (AurkB/C) to facilitate correct kinetochore-microtubule (KT-MT) attachment. In meiosis I in oocyte, we found that PP2Ac deficiency destabilized KT-MT attachments. Chemical inhibition of AurkB/C in PP2Ac-null oocytes partly restored the formation of lateral/merotelic KT-MT attachments but not correct KT-MT attachments. Taken together, our findings demonstrate that PP2Ac are essential for chromosome alignments and regulate the formation of correct KT-MT attachments in meiosis I in oocytes.

### ARTICLE HISTORY

Received 19 November 2015  
Revised 21 March 2016  
Accepted 31 March 2016

### KEYWORDS

fertility; KT-MT attachment; meiosis; oocyte; PP2A





### Introduction

Female meiosis in mammals is a complex process and prone to have segregation errors. After entering meiosis, oocytes need to be arrested at prophase I for a long period of time (weeks to months in mice, decades in human) before meiotic resumption. Interruption of prophase I arrest may lead to precocious meiotic resumption and depletion of oocyte stock.<sup>1</sup> The cohesin complex that holds sister chromatids together is seldom renewed and deteriorates with age during prophase I arrest, which may lead to precocious chromatid separation.<sup>2–4</sup> Due to error-prone chromosome-microtubule interactions and permissive spindle assembly checkpoint control, the misalignment of chromosomes cannot be efficiently corrected in oocyte meiotic division.<sup>5</sup>

Reversible protein phosphorylation plays important roles in a wide range of cellular processes. PP2A is a major serine/threonine protein phosphatase in eukaryotic cells. The PP2A holoenzyme consists of a 36 kDa catalytic subunit (C subunit, PP2Ac), a 65 kDa structural scaffolding subunit (A subunit, PR65) and a regulatory B subunit.<sup>6</sup> Each PP2A subunit has several isoforms; thus, different holoenzyme composition can exert specific functions in different cell types. In mammalian cells, the 2 isoforms of the C subunit of PP2A, PP2A $\alpha$  and PP2A $\beta$ , are encoded by the *Ppp2ca* gene and *Ppp2cb* gene, respectively.


Both isoforms consist of 309 amino acids and share 97% sequence similarity. In most human tissues, *Ppp2ca* is expressed at a higher abundance than *Ppp2cb*.<sup>7</sup> Tissue specific loss of *Ppp2ca* in the liver and heart causes severe physiological abnormalities, indicating that the functions of PP2A $\alpha$  cannot be compensated by PP2A $\beta$ .<sup>8–12</sup> The PP2Ac are highly expressed in the ovary<sup>7</sup> and whether PP2A $\alpha$  and PP2A $\beta$  are mutual independent in oocyte growth and maturation is unknown.

*In vitro* studies suggest that PP2A participates in multiple events during the meiotic maturation of oocytes. Meiotic resumption, also known as germinal vesicle break down (GVBD) in mouse oocytes, marks the entry of meiotic maturation. After GVBD, bivalent alignment generally occurs simultaneously with acentrosomal spindle formation in oocytes during meiosis I. At the early stage of meiosis I, when bivalents are individualized and move to the surface of the microtubule ball, microtubule organizing centers (MTOCs) are ejected from the center of the microtubule ball. Then, the bivalents are congressed at the middle of the spindle, MTOCs progressively clusters to form 2 dominant poles, and a bipolar spindle axis is established. At the late stage of meiosis I, bivalents are progressively stretched and form the equator plate in the middle of the spindle. The correct KT-MT attachment is formed and stabilized on fully stretched bivalents.<sup>5,13–15</sup> At the end of meiosis I,

**CONTACT** Xiang Gao  [gaoxiang@nju.edu.cn](mailto:gaoxiang@nju.edu.cn)  Model Animal Research Center, Nanjing University, 12 Xuefu Road, Nanjing 210061, China; Zhaoyu Lin  [linzy@nicemice.cn](mailto:linzy@nicemice.cn)  Model Animal Research Center, Nanjing University, 12 Xuefu Road, Nanjing 210061, China.

Color versions of one or more of the figures in this article can be found online at [www.tandfonline.com/kccy](http://www.tandfonline.com/kccy).

<sup>#</sup>Contributed equally to this work.

 Supplemental data for this article can be accessed on the publisher's website.

cohesins along the chromosome arms are cleaved by separase whereas centromeric cohesin is not cleaved, then all bivalents are segregated synchronously.<sup>16</sup> Interestingly, during mouse oocyte maturation, the activity of PP2A oscillates: it increases in prometaphase I and prometaphase II.<sup>17</sup> Inactivation of PP2A by OA treatment or RNAi disturbs multiple events in oocyte meiosis, including GVBD, spindle assembly, chromosome segregation and cytokinesis.<sup>18–23</sup> How PP2A regulate female fertility, cannot be confirmed by *in vitro* research methods. Using genetically modified mouse model to study the *in vivo* roles of PP2A could provide more reliable evidence.<sup>24</sup>

The risk of trisomic pregnancies increases with female age, the vast majority of human aneuploidies, such as Down's syndrome, result from segregation errors in female meiosis I.<sup>25</sup> Meiosis I in oocytes can be disrupted by OA treatment but the regulation of PP2A in dynamic spindle assembly and chromosome alignment during this stage, are not clear. In mitosis, sister KTs are bioriented to segregate sister chromatids (univalent). However, in meiosis I, sister KTs are monooriented to segregate homologous chromosome (bivalent). Previous studies have shown that PP2A can be recruited to KTs to facilitate correct KT-MT attachments formation both in mitosis and meiosis.<sup>14,26–28</sup> However, how PP2A regulate KT-MT attachments in oocyte meiosis I remains elusive.

To investigate the *in vivo* role of PP2A in oocytes maturation and female fertility, we established a mouse model in which the catalytic subunits of PP2A were specifically deleted

in oocytes. We found that each PP2Ac isoform could support female fertility independently. We demonstrated that the PP2Ac $\alpha$  and PP2Ac $\beta$  were essential for bivalent congression, bivalent stretching and the stabilization of lateral/merotelic KT-MT attachments during meiosis I in oocyte.

## Results

### Deleting both PP2Ac $\alpha$ and PP2Ac $\beta$ in oocytes caused female infertility

PP2Ac exists in 2 isoforms that are encoded by the *Ppp2ca* gene and *Ppp2cb* gene. To inactivate PP2A in mouse oocytes at the early stage of oocyte growth, we deleted *Ppp2ca* and *Ppp2cb* specifically in oocytes using *Zp3-Cre* transgenic mice in which Cre recombinase is expressed in the oocytes at primary follicular stages (Supplementary information, Figure S1A).<sup>29</sup> The resulting *Ppp2ca*<sup>fl/fl</sup>:*Zp3-Cre* females and *Ppp2cb*<sup>fl/fl</sup>:*Zp3-Cre* females were normally fertile, but *Ppp2ca*<sup>fl/fl</sup>:*Ppp2cb*<sup>fl/fl</sup>:*Zp3-Cre* double knockout (DKO) females were infertile (Fig. 1A). Thus, only the loss of both PP2Ac $\alpha$  and PP2Ac $\beta$  in oocytes caused female infertility.

Hematoxylin-eosin (HE) staining on ovary sections from 3-wk-old, 9-wk-old and 27-wk-old female mice showed no apparent morphological difference between DKO and Ctrl mice (Supplementary information, Figure S1B). Ovaries from DKO females harbored a normal number of GV stage oocytes after PMSG

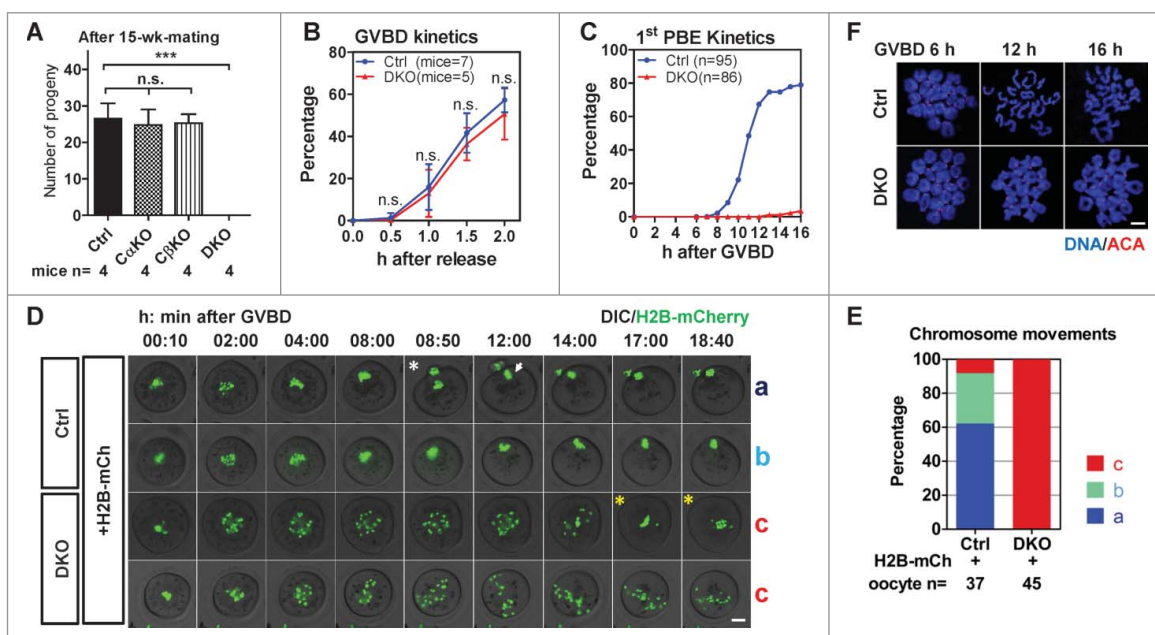


**Figure 1.** Loss of PP2Ac in oocytes caused female infertility and bivalent segregation failure in meiosis I. (A) 6-wk-old female mice were mated with wild-type male C57BL/6J mice for 15 wks. Cumulative number of pups between Ctrl, *Ppp2ca*<sup>fl/fl</sup>:*Zp3-Cre* (*Ca* KO), *Ppp2cb*<sup>fl/fl</sup>:*Zp3-Cre* (*Cb* KO) and DKO females were compared (mean  $\pm$  SD). Experiments were repeated twice and representative result is shown. Numbers of female mice were indicated. (B) DKO oocytes had normal GVBD kinetics. The percentage of oocytes that had undergone GVBD was scored every 0.5 h after release from IBMX (mean  $\pm$  SD). Experiments were repeated 3 times and a representative result is shown. The numbers of mice are indicated. (C) Oocytes from DKO mice could not extrude 1<sup>st</sup> PBs. Kinetics of 1<sup>st</sup> PBE after GVBD are shown. Oocytes that had undergone GVBD within 1.5 h after release into IBMX-free medium were selected for further culture. 1<sup>st</sup> PBE was scored every 1 h. Data were collected from 3 independent experiments. The numbers of oocytes are indicated. (D) Chromosomes failed to segregate in DKO oocytes. Still images with times from representative live imaging series are shown. The DIC (differential interference contrast) channel and H2B-mCherry channel were merged together. Genotypes of oocytes and injected mRNA (H2B-mCh for H2B-mCherry) are indicated. Types of chromosome movements are labeled on the right side of each series. Time is shown in h:min after GVBD. The white asterisk indicates the chromosome segregation in Ctrl oocytes; the white arrow indicates the metaphase II plate; yellow asterisks indicate unstable chromosome alignment in DKO oocytes. Bar = 20  $\mu$ m. (E) Comparison of the frequencies of different types of chromosome segregation in oocytes. The numbers of oocytes used for analysis are indicated. Data were collected from 3 independent experiments. (F) Bivalents failed to separate in DKO oocytes after GVBD. Chromosome spreads were prepared from the indicated time after GVBD and immunostained for DNA and centromeres (ACA, anti-centromere antibodies). Bar = 5  $\mu$ m. Statistics: n.s., no significant difference; \*\*\*,  $P < 0.001$ .

stimulation (Supplementary information, Figure S1C and S1D). Immunoblotting on GV stage oocytes and immunofluorescence on chromosome spreads confirmed the absence of PP2Ac proteins in DKO oocytes<sup>30</sup> (Supplementary information, Figure S1E and F). Ovaries from DKO females exhibited superovulatory responses normally after induction but the 1<sup>st</sup> polar body extrusion (PBE) rate in the DKO eggs was low (Supplementary information, Figure S1G-I). To explore preimplantation embryonic development, 24-day-old DKO and Ctrl females were mated with wild type males after superovulation, and embryos were isolated from the oviduct 1.5 d post coitum (dpc). In the embryos from Ctrl females, 66.3% had reached the 2-cell stage, 5.5% had degenerated and 28.2% were undivided (including oocytes, unfertilized eggs, and fertilized eggs that had not undergone the 1<sup>st</sup> mitotic division). In the embryos from DKO females, no 2-cell stage embryos were found, 62.4% had degenerated and 37.6% were undivided cells (Supplementary information, Figure S1J and S1K). Thus, DKO females could not produce functional zygotes to develop into normal embryos. These results demonstrated that deleting PP2Ac in primary follicular stage oocytes did not affect ovarian functions but produced defective oocytes, leading to female infertility.

### **Oocytes lacking PP2Ac failed to segregate bivalents in meiosis I**

DKO females were infertile due to the defective oocytes in which the 1<sup>st</sup> PBE seldom happen; thus, we focused on the meiotic maturation process in DKO oocytes. We isolated oocytes from mouse ovaries and examined the GVBD kinetics which marks the meiotic resumption of oocyte. Previous studies have shown that PP2A can inhibit GVBD in mouse oocytes.<sup>18,19</sup> We found that DKO oocytes showed indistinguishable GVBD kinetics compared to Ctrl oocytes when they were cultured in M2 medium (Fig. 1B). Then, we examined the 1<sup>st</sup> PBE kinetics which marks meiosis I exit in oocytes. In 67.4% of Ctrl oocytes, 1<sup>st</sup> PBE occurred before 12 h after GVBD (GVBD 12 h). However, in DKO oocytes, no 1<sup>st</sup> PBE occurred at GVBD 12 h; at GVBD 16 h, only 3.5% of DKO oocytes had extruded 1<sup>st</sup> polar bodies (PBs) (Fig. 1C). Thus, the PP2Ac deficiency did not affect meiotic resumption but caused 1<sup>st</sup> meiotic division failure.

The failure to extrude 1<sup>st</sup> PBs prompted us to investigate the process of chromosome segregation in DKO oocytes. To visualize chromosome movements in oocytes, we injected GV stage oocytes with histone H2B-mCherry mRNA (0.4 pg/pl) and followed chromosome movements by time-lapse epifluorescence microscopy. Oocytes expressing H2B-mCherry that had undergone GVBD within 1.5 h after release from IBMX were chosen for analysis. We distinguished 3 predominant phenotypes of chromosome movements: align before GVBD 8 h and segregate before GVBD 12 h (type 'a'); align GVBD 8 h but could not segregate (type 'b'); neither align before GVBD 8 h nor segregate (type 'c'). In Ctrl oocytes, the proportion of the 3 phenotypes was 62.2%, 29.7% and 8.1%, respectively. In contrast, 100% of the DKO oocytes showed phenotype 'c' (Fig. 1D and E). In most Ctrl oocytes, chromosomes individualized, congressed, aligned and segregated normally (Fig. 1D, series 1, type 'a'; Supplementary information, Video 1). However, in DKO oocytes, although chromosomes could individualize, they could not

congress. Chromosomes in DKO oocytes continued moving and became scattered in the ooplasm. (Fig. 1D, series 4, type 'c'; Supplementary information, Video 1). In some DKO oocytes, at a very late time (> GVBD 12 h), chromosomes were unstably aligned. In these oocytes with unstably aligned chromosomes, the aligned chromosomes dispersed later (Fig. 1D, series 3, type 'c', yellow asterisks; Supplementary information, Video 1). Immunostaining on the chromosome spreads showed that the Ctrl oocyte chromosomes remained as bivalents at GVBD 6 h and were segregated to univalents after GVBD 12 h. However, in the DKO oocytes, the chromosomes remained as bivalents up to 16 h after GVBD (Fig. 1F).

To confirm whether the chromosome segregation defects in DKO oocytes resulted from the PP2Ac deficiency, we evaluated whether the complementation of PP2Ac in GV stage DKO oocytes would recover the defects. We injected mRNAs encoding PP2Ac $\alpha$  (0.1 pg/pl), PP2Ac $\beta$  (0.01 pg/pl) and H2B-mCherry (0.2 pg/pl) to complement PP2Ac in DKO oocytes (DKO+PP2Ac). Meanwhile, a group of DKO oocytes were only injected with H2B-mCherry mRNA as the control. Complementation of PP2Ac recovered the proportions of the 'a' and 'b' phenotypes in the DKO+PP2Ac oocytes (Supplementary information, Figure S2A and S2B; Supplementary information, Video 2). The proportions of the 'a' or 'b' phenotype in DKO+PP2Ac oocytes did not reach the levels in Ctrl oocytes, which might be due to the different expression levels of the injected mRNAs. After live microscopy, oocytes were collected, and the complementation of PP2Ac in DKO+PP2Ac oocytes was confirmed by immunoblotting (Supplementary information, Figure S2C). From these results we found that the bivalents in DKO oocytes failed to align or segregate in meiosis I.

### **Chromosome alignment and spindle formation were disrupted in DKO oocytes**

To determine chromosome alignment in the spindle, we simultaneously immunostained chromosomes and microtubules in oocytes. Consistent with the results from time lapse microscopy, in most of the Ctrl oocytes, bipolar spindles had formed at GVBD 4 h; chromosomes had aligned in the middle of the spindles and formed metaphase I plates at GVBD 6 h; and chromosomes had segregated and metaphase II plates had formed at GVBD 12 h (Fig. 2A, upper row). However, chromosomes were persistently scattered in the spindles in most of the DKO oocytes (Fig. 2A, lower row). Multipolar spindles appeared in some DKO oocytes (Fig. 2A, yellow asterisks). We set a criterion to classify chromosome alignments into aligned, segregated, severely misaligned and mildly misaligned according to the chromosome distribution in the spindle (Fig. 2B). At GVBD 8 h, chromosomes had aligned in 96.6% of Ctrl oocytes, whereas chromosomes were severely misaligned in 91.0% of DKO oocytes. At GVBD 16 h, chromosomes had segregated in 79.3% of Ctrl oocytes, whereas chromosomes were severely misaligned in 69.1% of DKO oocytes or mildly misaligned in 19.8% of DKO oocytes (Fig. 2C). Moreover, spindles elongated more in DKO oocytes (Supplementary information, Figure S3B), in agreement with previous studies.<sup>21,24</sup> Note that at GVBD 8 h and GVBD 16 h, chromosomes were aligned in 1.1% and 8.6% of the DKO oocytes, respectively. These DKO

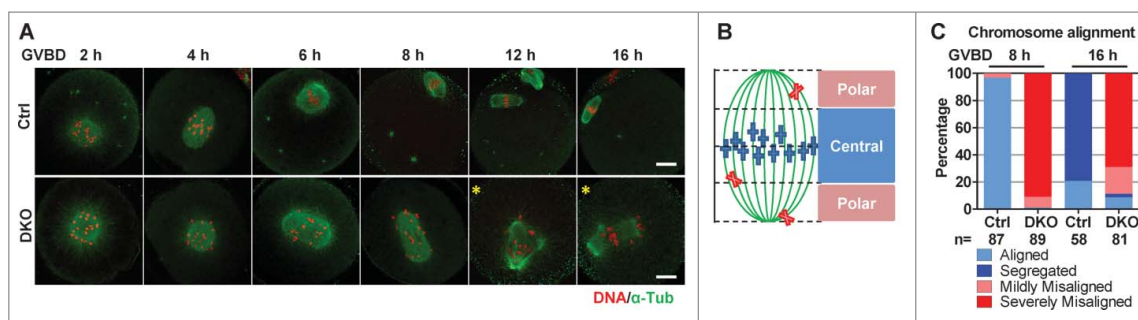


**Figure 2.** Bivalents were severely misaligned in DKO oocytes. (A) Bivalents in DKO oocytes were misaligned after GVBD. Oocytes were fixed at the indicated times after GVBD and immunostained for DNA and  $\alpha$ -tubulin. Representative z-projected confocal images are shown. The yellow asterisks indicate the DKO oocytes containing multipolar spindles. Bar = 20  $\mu$ m. (B) Cartoon showing the possible chromosome distribution in a spindle during meiosis I. Spindle area was 1:2:1 divided into a central region and the 2 flanking polar regions. Four different Chromosome alignments were distinguished: chromosomes aligned inside the central region (defined as ‘aligned’); no more than 6 chromosomes distributed in the polar regions (defined as ‘mildly misaligned’); more than 6 chromosomes distributed in the polar regions (defined as ‘severely misaligned’); chromosomes were separated (defined as ‘segregated’). (C) Chromosomes in the majority of DKO oocytes were severely misaligned after GVBD. The frequencies of 4 types of chromosome alignments in Ctrl and DKO oocytes at GVBD 8 h and GVBD 16 h are shown. The numbers of oocytes used for analysis are indicated. Data were collected from 3 independent experiments

oocytes may correspond to the DKO oocytes with unstably aligned chromosomes that were observed in the live microscopy experiments (Fig. 1D, series 3; Supplementary information, Video 1).

Mammalian oocytes lack conventional centrosomes during meiotic division.<sup>31</sup> In mouse oocyte meiosis I, MTOCs functionally replace centrosomes, and progressively organize into a bipolar intermediate to establish the bipolar spindle and chromosome biorientation.<sup>13,32</sup> Some of the DKO oocytes contained bipolar spindles although the chromosomes were misaligned, so we wondered whether the self-organization of MTOCs was affected in DKO oocytes. MTOCs were indicated by the location of  $\gamma$ -tubulin. At 2 h after GVBD, multiple MTOC foci had emerged on the surface of the microtubule ball in both Ctrl and DKO oocytes. In Ctrl oocytes, at GVBD 6 h and GVBD 8 h, multiple MTOCs poles had clustered into 2 bipolar dominant poles in the spindle (Supplementary information, Figure S3A, white arrows). However, in DKO oocytes, MTOCs were persistently fragmented and distributed in the spindle, no dominant MTOCs clusters had emerged before GVBD 8 h, even in the bipolar spindles (Supplementary information, Figure S3A). At GVBD 8 h and GVBD 16 h, dominant MTOC clusters emerged but were not bipolar in the spindles of some DKO oocytes (Supplementary information, Figure S3A, yellow arrows). From these data we demonstrated that the self-organization of MTOCs was disrupted in DKO oocytes. Thus, the PP2Ac are required for proper chromosome alignment and acentrosomal spindle formation during meiosis I in mouse oocytes.

### Loss of bivalent stretching and stable KT-MT attachments in DKO oocytes

In oocyte meiosis I, bivalent stretching is coupled with the alignment of bivalents. After fully stretching bivalents, stable KT-MT attachments increases.<sup>5,14</sup> The loss of PP2Ac caused severe chromosome misalignment in the spindle, which indicated the absence of stable and balanced forces on bivalents. To monitor the biorientation and stretching of bivalents in oocytes during meiosis I, we analyzed the inter-KT distances at 2, 4, 6, and 8 h after GVBD. In Ctrl oocytes, we found an increasing proportion of bioriented bivalents (Fig. 3A), and the mean inter-KT

distance increased after GVBD and peaked at GVBD 6 h (Fig. 3B,  $4.7 \pm 1.0 \mu$ m). However, in DKO oocytes, only a few bivalents were bioriented (Fig. 3A). Most of the bivalents in DKO oocytes remained weakly stretched, although the mean inter-KT distance gradually increased from GVBD 2 h to GVBD 8 h (Fig. 3B,  $1.5 \pm 1.0 \mu$ m to  $2.7 \pm 1.4 \mu$ m). Therefore, the proportion of bioriented and stretched bivalents remained low in DKO oocytes.

To determine the stability of the KT-MT attachments, we treated oocytes on ice to depolymerize the dynamic non-stable microtubules. After ice treatment, the KT-MT attachments were categorized into 3 types. KTs that had no contact with MT bundles or contacted short MT bundles from multiple directions were defined as “no attachment” (Fig. 3C, red panes); KTs that attached to the side of the MT bundles or attached to 2–3 different microtubules from different directions were defined as “lateral/merotelic attachment” (Fig. 3C, green panes); and KTs that attached to one end of the microtubules were defined as “correct attachment” (Fig. 3C, blue panes). In Ctrl oocytes, from GVBD 4 h to 8 h, correct attachments substantially increased. However, in most of the DKO oocytes, coupled with the severe misalignment of bivalents, most of the KTs were unattached from GVBD 2 h to GVBD 16 h (Fig. 3C and D). The DKO oocytes whose bivalents had aligned or were mildly misaligned at GVBD 16 h corresponded to DKO oocytes with unstably aligned chromosomes (Fig. 1D, series 3; Supplementary information, Video 1), and bivalents were not well stretched or bioriented in them (Supplementary information, Fig. S4). Those oocytes also contained few correct KT-MT attachments (Fig. 3C and D, mildly misaligned DKO oocytes at GVBD 16 h). Therefore, the PP2Ac are required for bivalent stretching and the stabilization of KT-MT attachments during meiosis I in oocytes.

### AurkB/C inhibition partly reversed the defects in DKO oocytes

AurkB/C phosphorylates components of KNL1/Mis12 complex/Ndc80 complex (KMN) network to regulate the stability of KT-MT attachments.<sup>33,34</sup> In both mitosis and meiosis, the phosphorylation level of the KMN network is negatively correlated with the stability of KT-MT attachments<sup>14,26,34</sup> (Fig. 4A–C). Using an antibody recognizing phosphorylated serine 24 in hKNL1,<sup>34</sup> we compared bivalents with similar

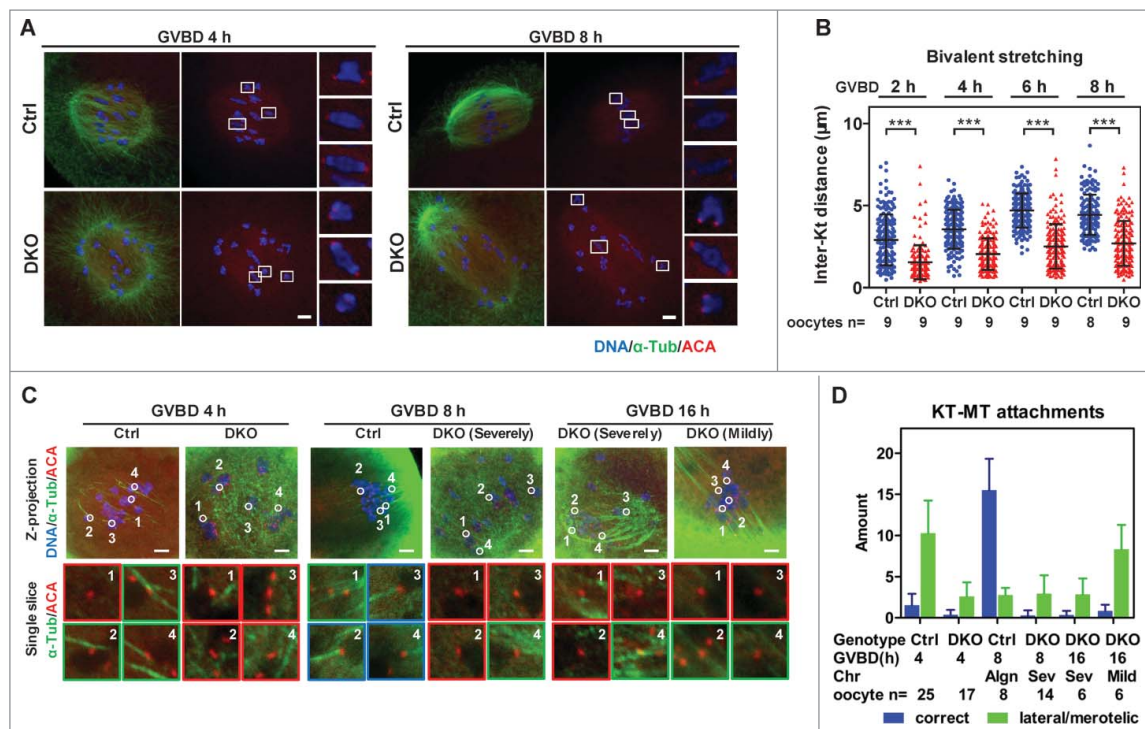


**Figure 3.** Lack of bivalent stretching and stable KT-MT attachments in DKO oocytes. (A) Oocytes were immunostained for DNA,  $\alpha$ -tubulin and KTs (Anti-centromere antibodies, ACA) to determine bivalent orientation and stretching. Representative z-projected confocal images of Ctrl and DKO oocytes at GVBD 4 h and GVBD 8 h are shown. Magnified views for 3 representative bivalents in each oocyte are shown in the right side of each z-projected image. Bar = 5  $\mu$ m. (B) Inter-KT distances of bivalents in DKO and Ctrl oocytes at indicated times after GVBD were plotted (mean  $\pm$  SD are shown). The numbers of oocytes used for analysis are indicated. Representative result from 3 independent experiments. (C) Oocytes at indicated time points were ice-treated and immunostained for DNA,  $\alpha$ -tubulin and KTs (ACA) to determine KT-MT attachments. Representative z-projected images of the whole spindles are shown in the upper row. Magnified views of the KT-MT attachments, indicated by circles and numbers in the upper row, from a single slice, are shown in the lower rows. The types of misalignment of DKO oocytes are indicated. Red panes indicate no attachment; Green panes indicate lateral/merotelic attachments; blue panes indicate correct attachments. Bar = 5  $\mu$ m. (D) KT-MT attachments in oocytes at times after GVBD were analyzed. Correct attachments (blue column) and lateral/merotelic attachments (green column) were scored (mean  $\pm$  SD). Chromosome alignments (Algn, aligned; Sev, severely misaligned; Mild, mildly misaligned), numbers of oocytes used for analysis are indicated. Representative result from 3 independent experiments. Statistics: \*\*\*,  $P < 0.001$ .

stretching (inter KT distance between 4 to 6  $\mu$ m) from DKO and Ctrl oocytes at GVBD 6 h and found that the fluorescence intensities of phosph-hKNL1-ser24 in KTs were increased by 1.3-fold in DKO oocytes (Fig. 4D and E). In addition, phosphorylation of Ser 10 in histone H3 (pH3s10), a well-known substrate of AurkB/C during mitosis and meiosis,<sup>35</sup> was increased by 2.6 and 3.6-fold at GVBD 4 h and 8 h respectively, in DKO oocytes (Fig. 3F and G). To determine whether the defects of KT-MT attachment, as well as the chromosome alignment in DKO oocytes, could be restored by suppressing AurkB/C activity, we treated oocytes with an AurkB/C inhibitor, hesperadin (250 nM), during meiotic maturation. After treatment, oocytes were immunostained and chromosome alignments were classified (Fig. 5A and B). In Ctrl oocytes, hesperadin treatment from GVBD 3 h to GVBD 5 h accelerated the alignment of chromosomes (Fig. 5B, from 16.1% to 30.3%, at GVBD 5 h); hesperadin treatment from GVBD 5 h to GVBD 9 h accelerated the extrusion of the 1<sup>st</sup> PBs (Supplementary information, Figure S5A and S5B, from 13.1% to 75.3%, at GVBD 9 h). Hesperadin treatment also caused mild misalignment in Ctrl oocytes, which was consistent with previous studies<sup>5,36</sup> (Fig. 5B, 9.7% to 18.2% at GVBD 5 h; Supplementary information, Figure S5B, 0% to 6.5% at GVBD 9 h). In DKO oocytes, hesperadin treatment from GVBD 5 h to 9 h decreased severely misaligned oocytes (Fig. 5B, from 91.6% to 60.4%) and increased the mildly misaligned oocytes (Fig. 5B, from 4.7% to

32.4%). However, the majority of DKO oocytes after hesperadin treatment were still severely misaligned (60.4%,  $n = 111$ ).

Next we analyzed bivalent stretching and KT-MT attachments in oocytes that had not extruded 1<sup>st</sup> PBs after hesperadin treatment (Figs. 5A and 6A). In Ctrl oocytes, compared with the untreated oocytes, hesperadin treatment from GVBD 3 h to 5 h had little effects on bivalents stretching (Fig. 5C,  $3.9 \pm 1.3 \mu$ m versus  $4.1 \pm 2.0 \mu$ m) but significantly increased the proportion of correct KT-MT attachments (Fig. 6B,  $1.8 \pm 0.4$  to  $12.5 \pm 7.6$ ). This result is consistent with previous studies.<sup>14,26,27</sup> In DKO oocytes, both the severely and mildly misaligned oocytes were analyzed. Compared with untreated DKO oocytes, hesperadin treatment from GVBD 5 h to GVBD 9 h significantly increased bivalent stretching, in both mildly and severely misaligned DKO oocytes (Fig. 5C, from  $3.1 \pm 1.3 \mu$ m to  $3.9 \pm 1.3 \mu$ m in mildly misaligned DKO oocytes, from  $2.7 \pm 1.2 \mu$ m to  $3.7 \pm 1.8 \mu$ m in severely misaligned DKO oocytes). Note that without hesperadin treatment, there were more stretched bivalents in the mildly misaligned DKO oocytes than in the severely misaligned DKO oocytes ( $3.1 \pm 1.3 \mu$ m vs.  $2.7 \pm 1.2 \mu$ m). After hesperadin treatment, the resulting mildly and severely misaligned DKO oocytes exhibited similar bivalent stretching ( $3.9 \pm 1.3 \mu$ m versus  $3.7 \pm 1.8 \mu$ m). Concomitant with the recovery of bivalent stretching, lateral/merotelic attachments significantly increased, to similar amounts, in both the mildly and severely misaligned DKO oocytes after hesperadin treatment (Fig. 6B, from  $14.0 \pm 4.6$  to

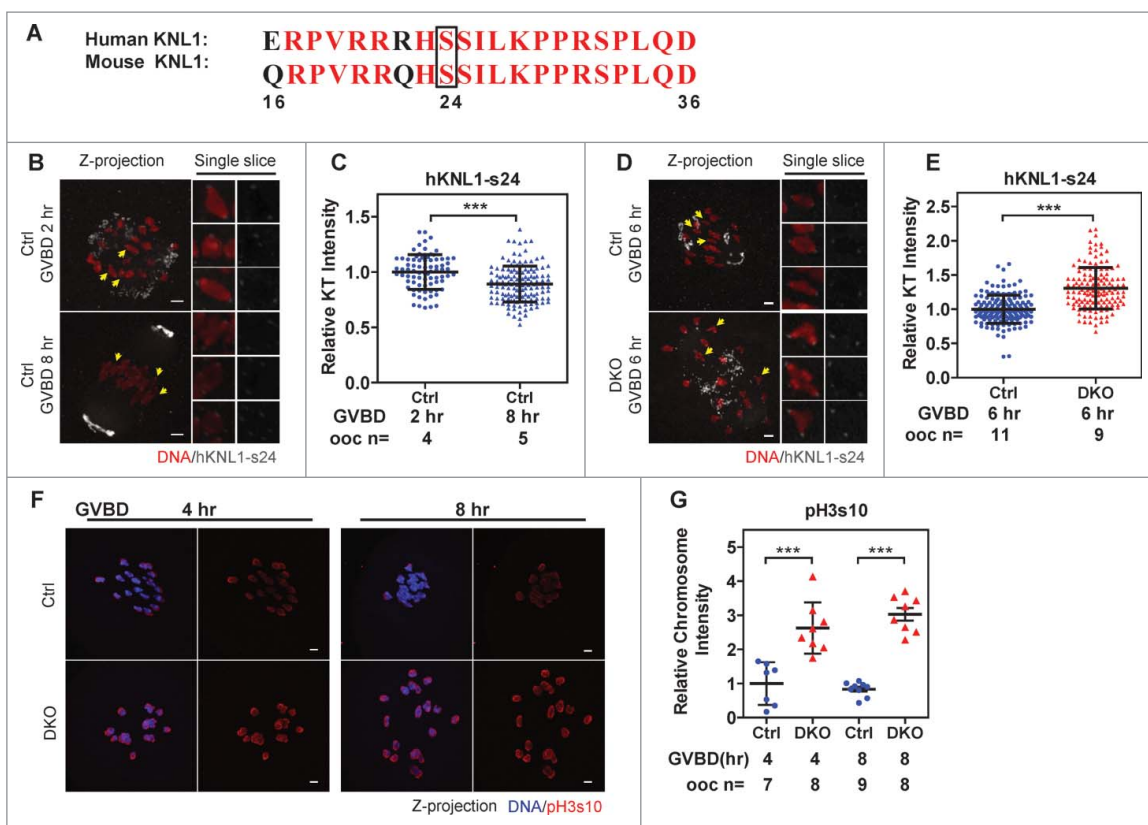


**Figure 4.** Phosphorylation of hKNL1-ser24 and pH3s10 were increased DKO oocytes. A polyclonal antibody recognizing the phosphorylated ser24 in hKNL1 protein (hKNL1-ser24) of KMN network has been developed based on the human protein sequences by Iain M. Cheeseman's group. (A) Similarity of the immunogenic peptide sequences of hKNL1-ser24 was compared between human and mouse. Identical residues are indicated in red font. The black box marks the Serine 24 phosphorylation site. (B) Feasibility of the antibody was evaluated in Ctrl oocytes. Ctrl oocytes were fixed at 2 h or 8 h after GVBD and immunostained for DNA and hKNL1-ser24. Representative z-projected images are shown in the left. Magnified views of the single chromosomes, indicated by the yellow arrows, from single slices are shown in the right panels. Note that the anti-hKNL1-ser24 antibody also targeted in the area of MTOCs. Bar = 5  $\mu$ m. (C) The anti-hKNL1-ser24 antibody is feasible for immunostaining mouse oocytes. Intensities of hKNL1-ser24 signals on KTs were normalized to the average of Ctrl oocytes at GVBD 2 h and plotted (mean  $\pm$  SD bars are shown). Numbers of oocytes used for analysis are indicated. Representative result from 3 independent experiments. (D) Oocytes were fixed at 6 h after GVBD and immunostained for DNA and hKNL1-ser24. Z-projected images of all the chromosomes are shown in the left panel. Magnified views of the representative single chromosomes, indicated by the yellow arrows, from single slices are shown in the right panels. Bar = 5  $\mu$ m. (E) The intensities of the hKNL1-ser24 signal on KTs were normalized to the average intensity of Ctrl oocytes at GVBD 6 h and plotted (mean  $\pm$  SD bars are shown). The numbers of oocytes used for analysis are indicated. Representative result from 3 independent experiments. (F) Oocytes were immunostained for DNA and pH3s10 at 4 h and 8 h after GVBD. Z-projected images of all the chromosomes are shown. Bar = 5  $\mu$ m. (G) The intensities of pH3s10 signal on Chromosome clusters were normalized to the average intensity of Ctrl oocytes at GVBD 4 h and plotted (mean  $\pm$  SD bars are shown). Representative result from 2 independent experiments. Statistics: \*\*\*,  $P < 0.001$ .

$23.8 \pm 2.2$  in mildly misaligned DKO oocytes, from  $4.9 \pm 3.8$  to  $21.2 \pm 6.7$  in severely misaligned DKO oocytes). However, correct attachments were not significantly increased after hesperadin treatments in DKO oocytes, even in the DKO oocytes whose bivalents were largely stretched (Fig. 6A, hesperadin treated DKO oocytes, mildly misaligned). From the above data, we conclude that the defects of chromosome alignment, bivalent stretching and lateral/merotelic KT-MT attachments caused by PP2Ac deficiency can be partly reversed by AurkB/C inhibition in oocytes.

## Discussion

### PP2Ac $\alpha$ and PP2Ac $\beta$ compensate each other to support oocyte maturation

Many *in vitro* studies have indicated that PP2A regulate several essential processes during meiotic maturation in oocytes. Using a genetically modified mouse model to delete the C subunits of PP2A in oocytes, we showed that the PP2Ac $\alpha$  are important for oocyte maturation and female fertility. The PP2Ac $\alpha$ -null zygote is embryonic

lethal, whereas the PP2Ac $\beta$ -null mouse has no obvious abnormality.<sup>10</sup> The function of PP2Ac $\beta$  has never been demonstrated. Previous studies have shown that *Ppp2ca* is expressed at a higher abundance than *Ppp2cb* in most human tissues<sup>7</sup> and the dominant functions of PP2Ac $\alpha$  cannot be compensated by PP2Ac $\beta$  in embryonic development, the liver, or the heart.<sup>8-12</sup> From our data, a single knockout of *Ppp2ca* or *Ppp2cb* in oocytes resulted in normal fertility, revealing that each PP2Ac could support oocyte maturation by itself. We suspect that PP2Ac $\beta$  may exist as a backup regulator for PP2Ac $\alpha$  to regulate cell division in both meiosis and mitosis, which can only be revealed when PP2Ac $\alpha$  and PP2Ac $\beta$  are simultaneously depleted. DKO females had normal ovary morphology and ovulation, indicating that oocyte specific loss of PP2A activity has few effects on follicular development, in agreement with a previous study in which PP2A-A $\alpha$  were deleted specifically in mouse oocytes.<sup>24</sup>

### PP2A is essential for chromosome alignment and spindle formation in meiosis I

Previous studies showed that inhibition of PP2A by OA or specifically deleting scaffold PP2A-A $\alpha$  facilitates GVBD in

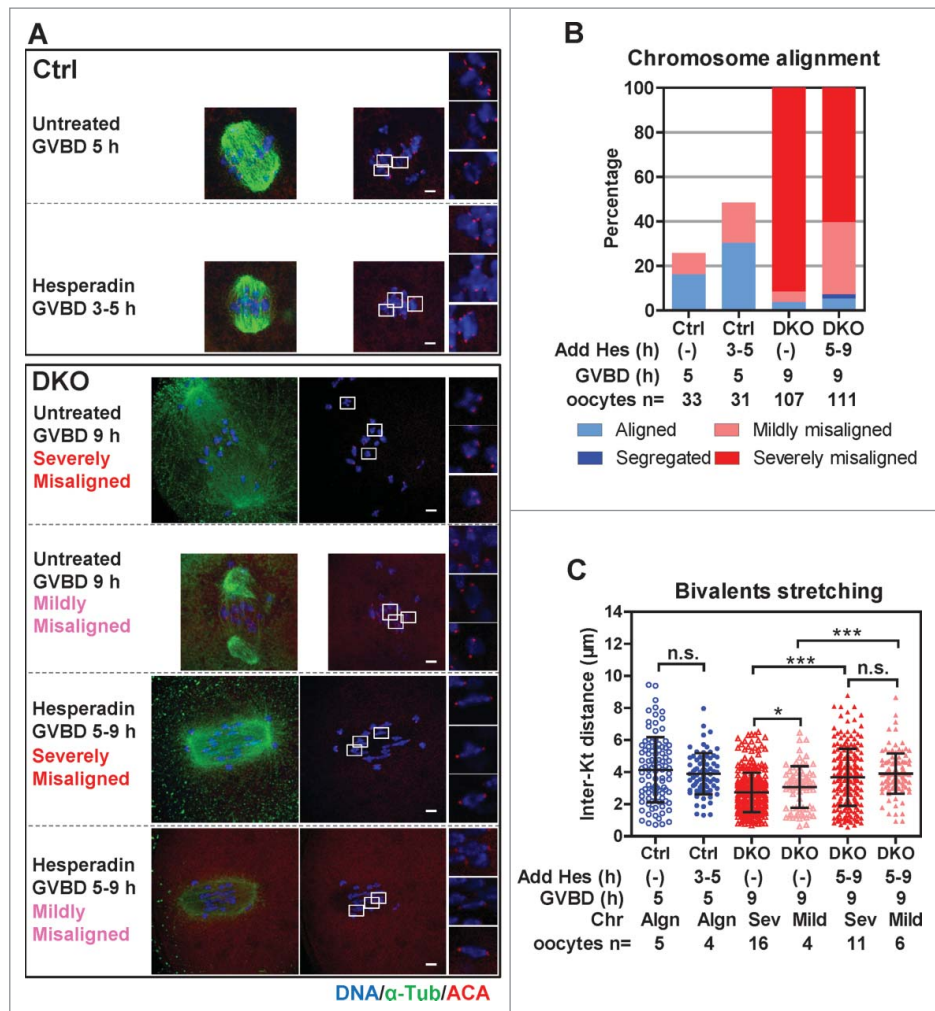


**Figure 5.** Hesperadin treatment partly recovered bivalent alignment and stretching in DKO oocytes. (A) Ctrl and DKO oocytes were treated with or without hesperadin (0.25  $\mu$ m) during indicated times after GVBD and then immunostained for DNA,  $\alpha$ -tubulin and KTs (ACA). Genotypes of oocytes, drug treatments and types of chromosome alignment are indicated. Representative z-projected images are shown, magnified views for 3 representative bivalents in each oocyte are shown in the right. Bar = 5  $\mu$ m. (B) After hesperadin treatments, oocytes were immunostained and analyzed. Chromosome alignments were classified according to Figure 2B. The histogram shows the frequencies of different types of chromosome alignment. Genotypes of oocytes, drug treatments and oocyte numbers are indicated. Data were collected from 3 independent experiments. (C) The inter-Kt distances of bivalents in Ctrl and DKO oocytes after hesperadin treatments were plotted (mean  $\pm$  SD are shown). Genotypes of oocytes, drug treatments, chromosome alignments (Algn, aligned; Sev, severely misaligned; Mild, mildly misaligned) and oocyte numbers are indicated. Representative result from 3 independent experiments. Statistics: n.s., no significant difference; \*,  $P < 0.05$ ; \*\*\*,  $P < 0.001$ .

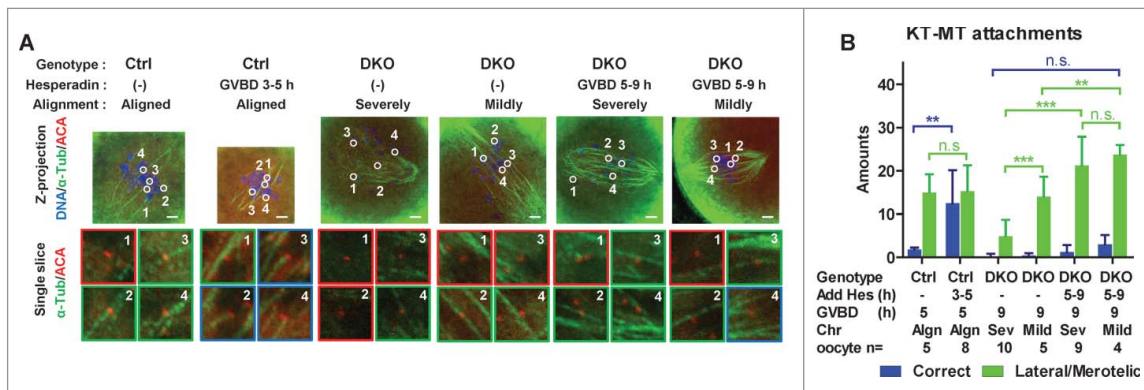


**Figure 6.** Hesperadin treatment partly restored lateral/merotelic KT-MT attachments in DKO oocytes. (A) After hesperadin treatment, oocytes were ice-treated and immunostained for DNA,  $\alpha$ -tubulin and KTs (ACA). Representative z-projected images of the whole spindles are shown in the upper row. Magnified views of the KT-MT attachments, indicated by circles and numbers in the upper panels, from a single slice, are shown in the lower rows. The types of misalignment of DKO oocytes are indicated. Green panes indicate the stable KT-MT attachments; red panes indicate the incorrect attachments. Genotypes, treatments and alignment types are indicated. Bar = 5  $\mu$ m. (B) KT-MT attachments in oocytes after hesperadin treatment were analyzed. Correct attachments (blue column) and lateral/merotelic attachments (green column) were scored (mean  $\pm$  SD). Chromosome alignments (Algn, aligned; Sev, severely misaligned; Mild, mildly misaligned), numbers of oocytes used for analysis are indicated. Representative result from 3 independent experiments. Statistics: n.s., no significant difference; \*\*,  $P < 0.01$ ; \*\*\*,  $P < 0.001$ .

oocytes,<sup>19,24,37,38</sup> and PP2A $\beta$  may play a key role in the meiotic arrest of oocytes.<sup>18,19</sup> In our study, the loss of PP2Acs did not significantly affect GVBD kinetics in oocytes under normal culture condition. It is worth determining whether DKO oocytes exhibit altered GVBD kinetics under challenging conditions. Generally, the dynamics of bivalent movement during meiosis I can be divided into 4 stages: individualization, congression, stretching and stabilization.<sup>5,14</sup> Due to PP2Ac deficiency in oocytes, bivalent individualization was retarded, congression did not occur, and the bivalents were in continuous misalignment and could not biorient. In a few DKO oocytes, the bivalents occasionally aligned but could not persist. In these chromosome-unstable-aligned DKO oocytes, the aligned bivalents were not bioriented or stretched by KT-MT attachments. The bivalents may be pushed to the central region of the spindles by an unstable interaction between MT and chromosome arm through MT and/or chromosome associated motor proteins. A recent study in mitosis suggests that PP2A regulate HSET to balance chromosome movement toward the metaphase plate.<sup>39</sup> It is worth determining whether HSET play a similar role in oocyte meiosis I.

OA treatment in oocytes prevents the formation of the spindle in meiosis I and rapidly disrupts the spindle in meiosis II.<sup>20,21</sup> In DKO oocytes, the microtubules were retained, but spindles were assembled incorrectly with abnormal MTOC self-organization. Interestingly, PP2A and AurkA co-localize to centrosomes in mitosis<sup>40</sup> and AurkA localizes to meiotic MTOCs and spindle poles in mouse oocytes.<sup>36,41-43</sup> PP2A dephosphorylate residue S51 in AurkA to promote AurkA degradation in mitosis.<sup>40</sup> Overexpression of AurkA is associated with supernumerary centrosomes and defective mitotic spindles in many types of solid tumor<sup>44</sup>; both overexpression and down regulation of AurkA cause incorrect spindle assembly in mouse oocytes.<sup>41,42</sup> Is it possible that PP2A regulate the self-organization of MTOCs to facilitate chromosome alignment and spindle assembly? What is the interplay between PP2A and AurkA in meiotic maturation of oocytes? These questions remain to be addressed. Note that in both mildly and severely misaligned DKO oocytes, dominant MTOC clusters emerged in the spindles at a late stage after GVBD (8–16 h), suggesting that the motor proteins responsible for MTOC clustering were still functional in DKO oocytes.<sup>13</sup> Besides, in DKO oocytes, degradation of securin, which is controlled by the spindle assembly checkpoint, was delayed (Supplementary information, Figure S3C).<sup>45</sup> The loss of scaffold subunit PP2A-A $\alpha$  in mouse oocytes compromised spindle shape and cytokinesis in meiosis II without affecting spindle formation during meiosis I.<sup>24</sup> Comparing with our results, the scaffold and catalytic subunits of PP2A appear to play different specific roles during meiotic maturation. Another possibility is that PP2A-A $\beta$  functionally compensates for PP2A-A $\alpha$  during oocyte meiosis I.

#### ***AurkB/C and PP2A counteract on stabilizing lateral/merotelic KT-MT attachments in meiosis I***

DKO oocytes lack stretched bivalents and stable KT-MT attachments, even in the minority whose bivalents were unstably aligned. Previous studies have shown that PP2A balances the activity of AurkB/C to regulate the formation of correct KT-MT attachment in mitosis, and the loss of correct KT-MT

attachments caused by decreasing the recruitment of PP2A to KTMs can be reversed by chemical inhibition of AurkB/C.<sup>26,27</sup> However, we found that inhibition of AurkB/C significantly restored lateral/merotelic attachments but not correct attachments in DKO oocytes. We also found that inhibition of AurkB/C partly restored the stretching of bivalents in both severely and mildly misaligned DKO oocytes. The discrepancies between previous studies in mitosis and our study in meiosis may be partially due to the technical reasons of knockdown efficiencies. In our DKO oocytes, PP2Ac was nearly absent; in previous mitosis models, the inactivation of PP2A by RNAi was not complete. The residual PP2A activity on KTMs after RNAi may be sufficient to promote correct KT-MT attachments formation when AurkB/C are inhibited by hesperadin in mitosis, which was not the same case in DKO oocytes. We speculate that that simultaneous inactivation of AurkB/C and activation of PP2A are required for the formation of correct KT-MT attachments. BubR1, an important component of the mitotic spindle assembly checkpoint, recruits PP2A to KTMs through its phosphorylated KARD domain to facilitate the formation of correct KT-MT attachments in both mitosis and meiosis.<sup>14,27</sup> In mitosis, the loss of stable KT-MT attachment caused by BubR1 knock down and overexpression of the BubR1-3A mutant (which cannot recruit PP2A to KTMs) can be reversed by AurkB/C inhibition<sup>27</sup>; in meiosis, artificially targeting of PP2A-B56 to KTMs restores KT-MT attachments in BubR1-3A-expressing oocytes during meiosis I.<sup>14</sup> However, in BubR1 knock out oocytes, the loss of correct KT-MT attachments are not restored by inhibiting AurkB/C but are restored by complementing cytosolic BubR1, which cannot localize to KTMs.<sup>28</sup> The mild rescue effects by AurkB/C inhibition on correct KT-MT attachment in DKO oocytes are similar to the phenomena in the BubR1 knock out oocytes, so we speculate that BubR1 can recruit PP2A to specific locations in ooplasm. Whether cytosolic PP2A, other than KT-localized PP2A, can regulate the formation of KT-MT attachment during meiotic maturation, remain to be addressed. Only upon bivalent stretching, AurkB/C inhibition can selectively stabilize correct KT-MT attachments in mouse oocytes.<sup>14</sup> From our data, in DKO oocytes after hesperadin treatment, correct KT-MT attachments did not increase correspondingly with increased bivalent stretching. Therefore, we conclude that PP2A and AurkB/C counteract each other on stabilizing lateral/merotelic KT-MT attachments in meiosis I of oocytes. We suspect that PP2A may be a key regulator in the conversion of the lateral/merotelic attachment to the correct attachment, which requires further investigation.

Many details regarding how reversible protein phosphorylation controls the meiotic maturation of oocytes remain elusive. Here, we found that the PP2Acs are essential for bipolar spindle formation and chromosome alignment in oocyte meiosis I. We demonstrated that PP2A regulates lateral/merotelic KT-MT attachment stability and bivalent stretching by counteracting AurkB/C. PP2A has been shown to participate in multiple key processes of mitosis; therefore, in addition to KT-MT attachment stability, many key processes in meiotic maturation should be regulated by PP2A. Using this knockout model, we can gain better insights into the mechanism by which reversible protein phosphorylation regulates meiotic maturation of oocytes.



## Materials and methods

### Mice

*Ppp2ca*<sup>fl/fl</sup> mice and *Ppp2cb*<sup>fl/fl</sup> mice were generated as previously described.<sup>10</sup> *Zp3-Cre* transgenic mice (Jackson laboratories) were crossed with *Ppp2ca*<sup>fl/fl</sup> mice and *Ppp2cb*<sup>fl/fl</sup> mice to obtain female *Ppp2ca*<sup>fl/fl</sup>:*Ppp2cb*<sup>fl/fl</sup>:*Zp3-Cre* mice, *Ppp2ca*<sup>fl/fl</sup>:*Zp3-Cre* mice and *Ppp2cb*<sup>fl/fl</sup>:*Zp3-Cre* mice for experiment. Female littermates without *Zp3-Cre* transgene were used as the controls. All the mice were in C57BL/6J genomic background. Mice were maintained in specific pathogen-free animal facility diet ad libitum. All animal welfare and experimental procedures were performed according to guidelines from the Animal Care and Use Committee of the Model Animal Research Center, Nanjing University.

### Fertility assay

Each 6-wk-old female mouse with indicated genotypes were bred to 9-wk-old C57BL/6J male mouse for a 15-wk period. During this period, the total number of pups produced by each female was recorded.

### Paraffin section and HE staining

Ovaries were isolated from females at indicated age and fixed in 4% (wt/vol) PFA (Sigma P6148) overnight, dehydrated in gradient ethanol, cleared by xylene and embedded in paraffin. Sections were done in 5  $\mu$ m per slice then deparaffinated in xylene, rehydrated in gradient ethanol, rinsed in distilled water, stained with hematoxylin for 6 min and eosin for 15 seconds, dehydrated in gradient ethanol and mounted with neutral resins.

### Isolation and culture of oocytes

3–4 wk female mice were i.p. injected with 5IU pregnant mare serum gonadotropin (PMSG, Sansheng Inc.) and 48 h later, fully grown GV-stage oocytes surrounded by cumulus cells were released from the ovaries by puncturing with 25-gauge needles in M2 medium (Sigma M7167) containing 20  $\mu$ M IBMX (Sigma I5879). GV stage oocytes were denuded by repetitive pipetting through a narrow-bore glass pipette. For further culture, oocytes were washed for 3 times and cultured in IBMX-free M2 medium drops covered with mineral oil (Sigma M8410) at 37°C.

### Microinjection and live imaging

mRNAs were synthesized using the Ultra T7 kit (Ambion AM1345) and purified using the RNeasy Mini Kit (Qiagen 74104). GV stage oocytes were arrested in M2 medium supplemented with 20  $\mu$ M IBMX, 5–10 pl mRNA was injected into each oocyte on a inverted microscope (Olympus, IX51) equipped with Eppendorf micromanipulators (Eppendorf, Transferrman 4r) and a microinjector (Eppendorf, FemtoJet 4i). After injection, oocytes were arrested for 2 h then released into IBMX free M2 medium. Oocytes expressing H2B-mCherry fluorescence and undergoing GVBD within 1.5 h after releasing

were selected for live imaging. Live imaging was done on an Olympus IX81 microscope equipped with a LUCPlanFLN 20X objective (0.45 NA), a X-Cite 120 excitation light source (EXCELITAS), a MIU-IBC heating stage at 37°C, a Retiga EXi Fast 1394 camera (QIMAGING). Live imaging was controlled by Image-Pro plus software (Media Cybernetics). Captured images were processed by using ImageJ software (NIH).

### Immunofluorescence and Confocal microscopy on oocytes

Oocytes at indicated stage were fixed in PHEM buffer (60 mM Pipes, 25 mM HEPES, 25 mM EGTA, 4 mM MgSO<sub>4</sub>, pH to 6.8) containing 4% (wt/vol) paraformaldehyde and 0.5% (vol/vol) TritonX-100 in at RT for 20min, permeabilized with 0.5% (vol/vol) TritonX-100 in PBS buffer at RT for 10min. For cold treatment, oocytes were transferred into pre-cooled M2 medium (containing corresponding concentration of hesperadin for the hesperadin treated oocytes) on ice and incubated for 10min before fixation. Incubations with primary antibody and secondary antibody were performed in blocking solution containing 7% (vol/vol) normal goat serum and 0.1% (vol/vol) Tween-20 in PBS buffer for 2 h at RT. Chromosomes were stained with Hoechst 33342 (Sigma B2261) for 20 min. The following primary antibodies were used for immunofluorescence:  $\alpha$ -tubulin (Sigma T5168), 1:500;  $\alpha$ -tubulin (Bioworld, bs501699), 1: 200;  $\gamma$ -tubulin (Sigma, T6557), 1:400, PP2Ac (CST 2038), 1:100; Anti-centromere antibodies (ACA, Fitzgerald, 90C-CS1058), 1:50; pH3s10 (CST 9701s), 1:200; hKNL1-ser24 (Gift from Iain M. Cheeseman group), 1:1000. The following Fluorescent conjugated secondary antibodies were used: Anti-Mouse IgG-FITC (Sigma, F5262), 1:200; Anti-Rabbit IgG-FITC (Sigma, F9887), 1:200; Anti-Rabbit IgG-Cy3 (sigma, C2306), Anti-Human IgG-FITC (Sigma, F9512). All the confocal microscopy images were taken at RT on a confocal laser scanning microscope (Olympus FV1000) equipped with a 60X oil objective (1.42 NA) by using FV10-ASW 4.0 software (Olympus). Interval between z-sections was 0.5  $\mu$ m. Z sections were analyzed and projected using FV10-ASW Viewer 2.0 software (Olympus).

### Drug treatment

For inhibiting AurkB/C in oocytes, Hesperadin (Selleck S1529) was prepared as stock solution in DMSO (Sigma D2650) at 10 mM then diluted to 250 nM in M2 medium for culture. For untreated controls, M2 medium containing equal concentration of DMSO was used. The duration of treatments were indicated in the text. Drug treated oocytes and untreated controls were cultured in separated dishes.

### Plasmid construction

For constructing H2B-mCherry expression vector: Coding sequence of mouse *Hist2h2be* gene (H2B) was cloned from mouse brain cDNA pool. Coding sequence of mCherry was cloned from pmCherry vector (Takara). H2B was fused to the N-terminal of mCherry via MluI restriction site and the resulting H2B-mCherry was inserted into XhoI-EcoRI restriction sites of pBluscriptIISK(+) vector (Invitrogen).

For constructing PP2Ac expression vectors: Coding sequence of mouse PP2Ac $\alpha$  and PP2Ac $\beta$  were cloned from mouse brain cDNA pool. Both of them were inserted into ClaI-EcoRI restriction sites of pBluscriptIIISK(+) vector respectively.

### Protein sample preparation and Western blotting

Denuded oocytes at indicated stage were transferred into lysis buffer containing 125 mM Tris (pH 6.8), 4% (wt/vol) SDS, 20% (wt/vol) glycerol, 10% (vol/vol)  $\beta$ -mercaptoethanol, 0.004% (wt/vol) bromophenol blue and heated to 100°C for 5 min.<sup>46</sup> Protein samples were separated in discontinuous Bis-Tris Gels (Invitrogen NP0316) followed by blotting onto PVDF membrane (Millipore IPVH00010). The following primary antibodies were used for western blot:  $\alpha$ -tubulin (Sigma T5168), 1:10,000;  $\beta$ -actin (Sigma A5441), 1:10,000; PP2Ac (CST 2038), 1:1,000; securin (Abcam, ab3305). The following secondary antibodies were used: HRP-conjugated goat anti-rabbit IgG (Sigma A9169), 1:20,000; HRP-conjugated goat anti-mouse IgG, (Pierce 31439), 1:20,000. The immuno-reactive bands were visualized with the immobilon western HRP Substrate (Millipore WBKLS0500).

### Chromosome spreading and Immunofluorescence

Chromosome spreads were prepared according to Ref. 30. Briefly, oocytes at indicated time points after GVBD were treated with Tyrode's acid (Sigma T1788) to remove the zona pellucida. The zona-pellucida-free oocytes were transferred into a drop of spreading solution (pH 9.2) containing 1% (wt/vol) paraformaldehyde, 0.15% (vol/vol) Triton X100 and 3 mM DTT on a glass slide. The drop was air dried at R.T. then used for immunostaining immediately or stored in -20°C. For immunofluorescence, chromosome spreads were washed in PBS buffer for 3 times, blocked in 3% (wt/vol) BSA, incubated with primary antibodies for 2 h at R.T., washed for 3 times, incubated with fluorescent conjugated secondary antibodies and Hoechst 33342 for 1 h, washed for 3 times and mounted in 50% (vol/vol) glycerol.

### Superovulation

Three-wk-old female mice were i.p. injected with 5 IU PMSG (Sansheng Inc.) and 48 h later with 5 IU hCG (Sansheng Inc.). Fourteen h after hCG injection, oviducts were isolated. The cumulus-cell-enclosed eggs were released from the oviducts in M2 medium containing 0.3 mg/ml hyaluronidase (sigma H4272) by incubating at 37°C for 5 min. After removing the cumulus cells, eggs were washed in M2 medium for further use.

### Isolation of 1.5 dpc embryos

In day 0, 3-wk-old female mice were i.p. injected with 5 IU PMSG (Sansheng Inc.) at 11:00 and 48 h later with 5 IU hCG (Sansheng Inc.). After then, each female mouse was 1:1 bred to a 9-wk-old male C57BL/6J mouse. On day 3 morning, vaginal plugs were checked and females who had vaginal plugs were selected for further use. On day 4 11:00 AM, which correspond to 1.5 dpc, oviducts were isolated from the female mice.

Embryos were flushed out from the oviducts and collected in M2 medium.

### Quantification of fluorescent intensities

Fluorescent intensities of the target on specific region (Ft) of the image were determined by ImageJ software (NIH) according to a previously reported method.<sup>47</sup> For each image, an inner region that includes the target of interest and the larger outer region including the inner region were selected. The total integrated fluorescence densities (Fi for inner, Fo for outer) and areas (Ai for inner, Ao for outer) were measured in each region. Ft was calculated through the formula:  $Ft = Fi - (Fo - Fi) * Ai / (Ao - Ai)$ . For quantification Ft on KT, a 20\*20 pixels inner region ( $\approx 1 \mu m^2$ ) and a 28\*28 pixels outer region ( $\approx 2 \mu m^2$ ) were manually selected around the best-in-focus image of each KT. For quantification Ft on Chromosomes, an inner region that includes all the chromosomes in and a 1.5-fold larger outer region covers the inner region were manually selected on the z-projected image of a oocyte.

### Statistical analysis

Two tailed, unpaired *t*-test was performed to compare the differences between groups. n.s., no significant difference; \*,  $P < 0.05$ ; \*\*,  $P < 0.01$ ; \*\*\*,  $P < 0.001$ .

### Abbreviations

ACA	anti-centromere antibodies
Aurk	Aurora kinase
dpc	day post coitum
GV	germinal vesicle
GVBD	germinal vesicle break down
KMN	KNL1/Mis12 complex/Ndc80 complex
KT-MT	kinetochores-microtubule
PB	polar body
PBE	polar body extrusion
pH3s10	phosphorylation of Ser 10 in histone H3
PP2A	protein phosphatase 2A
PP2Ac	catalytic subunit of protein phosphatase 2A

### Disclosure of potential conflicts of interest

No potential conflicts of interest were disclosed.

### Acknowledgments

We thank Dr. Iain M. Cheeseman for kindly providing antibodies and Drs. Xingxu Huang, Xueliang Zhu, Youqiang Su, Dong Zhang for their helpful suggestions. We thank Honglan Xue for assistance of the experiments.

### Funding

This work was supported by the Ministry of Science and Technology of China (grants 2014BAI02B01 and 2015BAI08B02), National Natural Science Foundation of China (grant 31301217) and Natural Science Foundation of the Jiangsu Higher Education Institutions of China (11KJB180010)

## References

- [1] Holt JE, Tran SM, Stewart JL, Minahan K, Garcia-Higuera I, Moreno S, Jones KT. The APC/C activator FZR1 coordinates the timing of meiotic resumption during prophase I arrest in mammalian oocytes. *Development* 2011; 138:905-13; PMID:21270054; <http://dx.doi.org/10.1242/dev.059022>
- [2] Jessberger R. Age-related aneuploidy through cohesion exhaustion. *EMBO Rep* 2012; 13:539-46; PMID:22565322; <http://dx.doi.org/10.1038/embor.2012.54>
- [3] Tachibana-Konwalski K, Godwin J, van der Weyden L, Champion L, Kudo NR, Adams DJ, Nasmyth K. Rec8-containing cohesin maintains bivalents without turnover during the growing phase of mouse oocytes. *Genes Dev* 2010; 24:2505-16; PMID:20971813; <http://dx.doi.org/10.1101/gad.605910>
- [4] Lister LM, Kouznetsova A, Hyslop LA, Kalleas D, Pace SL, Barel JC, Nathan A, Floros V, Adelfalk C, Watanabe Y, et al. Age-related meiotic segregation errors in mammalian oocytes are preceded by depletion of cohesin and Sgo2. *Curr Biol* 2010; 20:1511-21; PMID:20817533; <http://dx.doi.org/10.1016/j.cub.2010.08.023>
- [5] Kitajima TS, Ohsugi M, Ellenberg J. Complete kinetochore tracking reveals error-prone homologous chromosome biorientation in mammalian oocytes. *Cell* 2011; 146:568-81; PMID:21854982; <http://dx.doi.org/10.1016/j.cell.2011.07.031>
- [6] Zolnierowicz S. Type 2A protein phosphatase, the complex regulator of numerous signaling pathways. *Biochem Pharmacol* 2000; 60:1225-35; PMID:11007961; [http://dx.doi.org/10.1016/S0006-2952\(00\)00424-X](http://dx.doi.org/10.1016/S0006-2952(00)00424-X)
- [7] Khew-Goodall Y, Hemmings BA. Tissue-specific expression of mRNAs encoding alpha- and beta-catalytic subunits of protein phosphatase 2A. *FEBS Lett* 1988; 238:265-8; PMID:2844601; [http://dx.doi.org/10.1016/0014-5793\(88\)80493-9](http://dx.doi.org/10.1016/0014-5793(88)80493-9)
- [8] Pan X, Chen X, Tong X, Tang C, Li J. Ppp2ca knockout in mice spermatogenesis. *Reproduction* 2015; PMID:25628439
- [9] Xian L, Hou S, Huang Z, Tang A, Shi P, Wang Q, Song A, Jiang S, Lin Z, Guo S, et al. Liver-specific deletion of Ppp2calpha enhances glucose metabolism and insulin sensitivity. *Aging (Albany NY)* 2015; 7:223-32; PMID:25888638
- [10] Gu P, Qi X, Zhou Y, Wang Y, Gao X. Generation of Ppp2Ca and Ppp2Cb conditional null alleles in mouse. *Genesis* 2012; 50:429-36; PMID:21998041; <http://dx.doi.org/10.1002/dvg.20815>
- [11] Chen W, Gu P, Jiang X, Ruan HB, Li C, Gao X. Protein phosphatase 2A catalytic subunit alpha (PP2Aalpha) maintains survival of committed erythroid cells in fetal liver erythropoiesis through the STAT5 pathway. *Am J Pathol* 2011; 178:2333-43; PMID:21514445; <http://dx.doi.org/10.1016/j.ajpath.2011.01.041>
- [12] Lu N, Liu Y, Tang A, Chen L, Miao D, Yuan X. Hepatocyte-specific ablation of PP2A catalytic subunit alpha attenuates liver fibrosis progression via TGF-beta1/Smad signaling. *Biomed Res Int* 2015; 2015:794862; PMID:25710025
- [13] Schuh M, Ellenberg J. Self-organization of MTOCs replaces centrosome function during acentrosomal spindle assembly in live mouse oocytes. *Cell* 2007; 130:484-98; PMID:17693257; <http://dx.doi.org/10.1016/j.cell.2007.06.025>
- [14] Yoshida S, Kaido M, Kitajima TS. Inherent Instability of Correct Kinetochore-Microtubule Attachments during Meiosis I in Oocytes. *Dev Cell* 2015; 33:589-602; PMID:26028219; <http://dx.doi.org/10.1016/j.devcel.2015.04.020>
- [15] Hached K, Xie SZ, Buffin E, Cladiere D, Rachez C, Sacras M, Sorger PK, Wassmann K. Mps1 at kinetochores is essential for female mouse meiosis I. *Development* 2011; 138:2261-71; PMID:21558374; <http://dx.doi.org/10.1242/dev.061317>
- [16] Kitajima TS, Kawashima SA, Watanabe Y. The conserved kinetochore protein shugoshin protects centromeric cohesion during meiosis. *Nature* 2004; 427:510-7; PMID:14730319; <http://dx.doi.org/10.1038/nature02312>
- [17] Winston NJ, Maro B. Changes in the activity of type 2A protein phosphatases during meiotic maturation and the first mitotic cell cycle in mouse oocytes. *Biol Cell* 1999; 91:175-83; PMID:10425704; [http://dx.doi.org/10.1016/S0248-4900\(99\)80040-9](http://dx.doi.org/10.1016/S0248-4900(99)80040-9)
- [18] Su YQ, Sugiura K, Sun F, Pendola JK, Cox GA, Handel MA, Schimenti JC, Eppig JJ. MARF1 regulates essential oogenic processes in mice. *Science* 2012; 335:1496-9; PMID:22442484; <http://dx.doi.org/10.1126/science.1214680>
- [19] Alexandre H, Van Cauwenberge A, Tsukitani Y, Mulnard J. Pleiotropic effect of okadaic acid on maturing mouse oocytes. *Development* 1991; 112:971-80; PMID:1718679
- [20] Lu Q, Dunn RL, Angeles R, Smith GD. Regulation of spindle formation by active mitogen-activated protein kinase and protein phosphatase 2A during mouse oocyte meiosis. *Biol Reprod* 2002; 66:29-37; PMID:11751260; <http://dx.doi.org/10.1095/biolreprod66.1.29>
- [21] Chang HY, Jennings PC, Stewart J, Verrills NM, Jones KT. Essential role of protein phosphatase 2A in metaphase II arrest and activation of mouse eggs shown by okadaic acid, dominant negative protein phosphatase 2A, and FTY720. *J Biol Chem* 2011; 286:14705-12; PMID:21383018; <http://dx.doi.org/10.1074/jbc.M110.193227>
- [22] Mailhes JB, Hilliard C, Fuseler JW, London SN. Okadaic acid, an inhibitor of protein phosphatase 1 and 2A, induces premature separation of sister chromatids during meiosis I and aneuploidy in mouse oocytes in vitro. *Chromosome Res* 2003; 11:619-31; PMID:14516070; <http://dx.doi.org/10.1023/A:1024909119593>
- [23] Qi ST, Wang ZB, Ouyang YC, Zhang QH, Hu MW, Huang X, Ge Z, Guo L, Wang YP, Hou Y, et al. Overexpression of SET-beta, a protein localizing to centromeres, causes precocious separation of chromatids during the first meiosis of mouse oocytes. *J Cell Sci* 2013; 126:1595-603; PMID:23444375; <http://dx.doi.org/10.1242/jcs.116541>
- [24] Hu MW, Wang ZB, Jiang ZZ, Qi ST, Huang L, Liang QX, Schatten H, Sun QY. Scaffold subunit Aalpha of PP2A is essential for female meiosis and fertility in mice. *Biol Reprod* 2014; 91:19; PMID:24899574; <http://dx.doi.org/10.1095/biolreprod.114.120220>
- [25] Morris JK, Mutton DE, Alberman E. Revised estimates of the maternal age specific live birth prevalence of Down's syndrome. *J Med Screen* 2002; 9:2-6; PMID:11943789; <http://dx.doi.org/10.1136/jms.9.1.2>
- [26] Foley EA, Maldonado M, Kapoor TM. Formation of stable attachments between kinetochores and microtubules depends on the B56-PP2A phosphatase. *Nat Cell Biol* 2011; 13:1265-71; PMID:21874008; <http://dx.doi.org/10.1038/ncb2327>
- [27] Suijkerbuijk SJ, Vleugel M, Teixeira A, Kops GJ. Integration of kinase and phosphatase activities by BUBR1 ensures formation of stable kinetochore-microtubule attachments. *Dev Cell* 2012; 23:745-55; PMID:23079597; <http://dx.doi.org/10.1016/j.devcel.2012.09.005>
- [28] Touati SA, Buffin E, Cladiere D, Hached K, Rachez C, van Deursen JM, Wassmann K. Mouse oocytes depend on BubR1 for proper chromosome segregation but not for prophase I arrest. *Nat Commun* 2015; 6:6946; PMID:25897860; <http://dx.doi.org/10.1038/ncomms7946>
- [29] de Vries WN, Binns LT, Fancher KS, Dean J, Moore R, Kemler R, Knowles BB. Expression of Cre recombinase in mouse oocytes: a means to study maternal effect genes. *Genesis* 2000; 26:110-2; PMID:10686600; [http://dx.doi.org/10.1002/\(SICI\)1526-968X\(200002\)26:2%3c110::AID-GENE2%3e3.0.CO;2-8](http://dx.doi.org/10.1002/(SICI)1526-968X(200002)26:2%3c110::AID-GENE2%3e3.0.CO;2-8)
- [30] Chambon JP, Touati SA, Berneau S, Cladiere D, Hebras C, Groeme R, McDougall A, Wassmann K. The PP2A inhibitor I2PP2A is essential for sister chromatid segregation in oocyte meiosis II. *Curr Biol* 2013; 23:485-90; PMID:23434280; <http://dx.doi.org/10.1016/j.cub.2013.02.004>
- [31] Dumont J, Desai A. Acentrosomal spindle assembly and chromosome segregation during oocyte meiosis. *Trends Cell Biol* 2012; 22:241-9; PMID:22480579; <http://dx.doi.org/10.1016/j.tcb.2012.02.007>
- [32] Clift D, Schuh M. A three-step MTOC fragmentation mechanism facilitates bipolar spindle assembly in mouse oocytes. *Nat Commun* 2015; 6:7217; PMID:26147444; <http://dx.doi.org/10.1038/ncomms8217>
- [33] Cheeseman IM, Chappie JS, Wilson-Kubalek EM, Desai A. The conserved KMN network constitutes the core microtubule-binding site of the kinetochore. *Cell* 2006; 127:983-97; PMID:17129783; <http://dx.doi.org/10.1016/j.cell.2006.09.039>
- [34] Welburn JP, Vleugel M, Liu D, Yates JR, 3rd, Lampson MA, Fukagawa T, Cheeseman IM. Aurora B phosphorylates spatially distinct

- targets to differentially regulate the kinetochore-microtubule interface. *Mol Cell* 2010; 38:383-92; PMID:20471944; <http://dx.doi.org/10.1016/j.molcel.2010.02.034>
- [35] Goto H, Yasui Y, Nigg EA, Inagaki M. Aurora-B phosphorylates Histone H3 at serine28 with regard to the mitotic chromosome condensation. *Genes Cells* 2002; 7:11-7; PMID:NOT\_FOUND; <http://dx.doi.org/10.1046/j.1356-9597.2001.00498.x>
- [36] Shuda K, Schindler K, Ma J, Schultz RM, Donovan PJ. Aurora kinase B modulates chromosome alignment in mouse oocytes. *Mol Reprod Dev* 2009; 76:1094-105; PMID:19565641; <http://dx.doi.org/10.1002/mrd.21075>
- [37] Smith GD, Sadhu A, Wolf DP. Transient exposure of rhesus macaque oocytes to calyculin-A and okadaic acid stimulates germinal vesicle breakdown permitting subsequent development and fertilization. *Biol Reprod* 1998; 58:880-6; PMID:9546716; <http://dx.doi.org/10.1095/biolreprod58.4.880>
- [38] Sun QY, Wu GM, Lai L, Bonk A, Cabot R, Park KW, Day BN, Prather RS, Schatten H. Regulation of mitogen-activated protein kinase phosphorylation, microtubule organization, chromatin behavior, and cell cycle progression by protein phosphatases during pig oocyte maturation and fertilization in vitro. *Biol Reprod* 2002; 66:580-8; PMID:11870061; <http://dx.doi.org/10.1095/biolreprod66.3.580>
- [39] Xu P, Virshup DM, Lee SH. B56-PP2A regulates motor dynamics for mitotic chromosome alignment. *J Cell Sci* 2014; 127:4567-73; PMID:25179604; <http://dx.doi.org/10.1242/jcs.154609>
- [40] Horn V, Thelu J, Garcia A, Albiges-Rizo C, Block MR, Viallet J. Functional interaction of Aurora-A and PP2A during mitosis. *Mol Biol Cell* 2007; 18:1233-41; PMID:17229885; <http://dx.doi.org/10.1091/mbc.E06-12-1152>
- [41] Saskova A, Solc P, Baran V, Kubelka M, Schultz RM, Motlik J. Aurora kinase A controls meiosis I progression in mouse oocytes. *Cell Cycle* 2008; 7:2368-76; PMID:18677115; <http://dx.doi.org/10.4161/cc.6361>
- [42] Ding J, Swain JE, Smith GD. Aurora kinase-A regulates microtubule organizing center (MTOC) localization, chromosome dynamics, and histone-H3 phosphorylation in mouse oocytes. *Mol Reprod Dev* 2011; 78:80-90; PMID:21274965; <http://dx.doi.org/10.1002/mrd.21272>
- [43] Yao LJ, Zhong ZS, Zhang LS, Chen DY, Schatten H, Sun QY. Aurora-A is a critical regulator of microtubule assembly and nuclear activity in mouse oocytes, fertilized eggs, and early embryos. *Biol Reprod* 2004; 70:1392-9; PMID:14695913; <http://dx.doi.org/10.1095/biolreprod.103.025155>
- [44] Nikonova AS, Astsaturov I, Serebriiskii IG, Dunbrack RL, Jr., Golemis EA. Aurora A kinase (AURKA) in normal and pathological cell division. *Cellular and molecular life sciences : CMLS* 2013; 70:661-87; PMID:22864622; <http://dx.doi.org/10.1007/s00018-012-1073-7>
- [45] Vogt E, Kirsch-Volders M, Parry J, Eichenlaub-Ritter U. Spindle formation, chromosome segregation and the spindle checkpoint in mammalian oocytes and susceptibility to meiotic error. *Mutat Res* 2008; 651:14-29; PMID:18096427; <http://dx.doi.org/10.1016/j.mrgentox.2007.10.015>
- [46] Su YQ, Rubinstein S, Luria A, Lax Y, Breitbart H. Involvement of MEK-mitogen-activated protein kinase pathway in follicle-stimulating hormone-induced but not spontaneous meiotic resumption of mouse oocytes. *Biol Reprod* 2001; 65:358-65; PMID:11466201; <http://dx.doi.org/10.1095/biolreprod65.2.358>
- [47] Hoffman DB, Pearson CG, Yen TJ, Howell BJ, Salmon ED. Microtubule-dependent changes in assembly of microtubule motor proteins and mitotic spindle checkpoint proteins at PtK1 kinetochores. *Mol Biol Cell* 2001; 12:1995-2009; PMID:11451998; <http://dx.doi.org/10.1091/mbc.12.7.1995>